Acta Crystallographica Section D
Biological Crystallography
ISSN 0907-4449

1.8 Å structure of murine GITR ligand dimer expressed in *Drosophila melanogaster* S2 cells

Kausik Chattopadhyay,[a] Udupi A. Ramagopal,[b] Stanley G. Nathenson[a,c]* and Steven C. Almo[b,d]*

[a]Department of Microbiology and Immunology, Albert Einstein College of Medicine, Bronx, New York 10461, USA, [b]Department of Biochemistry, Albert Einstein College of Medicine, Bronx, New York 10461, USA, [c]Department of Cell Biology, Albert Einstein College of Medicine, Bronx, New York 10461, USA, and [d]Department of Physiology and Biophysics, Albert Einstein College of Medicine, Bronx, New York 10461, USA

Correspondence e-mail: nathenso@aecom.yu.edu, almo@aecom.yu.edu

Received 16 January 2009
Accepted 17 February 2009

PDB Reference: murine GITR ligand dimer, 3fc0, r3fc0sf.

Glucocorticoid-induced TNF receptor ligand (GITRL), a prominent member of the TNF superfamily, activates its receptor on both effector and regulatory T cells to generate critical costimulatory signals that have been implicated in a wide range of T-cell immune functions. The crystal structures of murine and human orthologs of GITRL recombinantly expressed in *Escherichia coli* have previously been determined. In contrast to all classical TNF structures, including the human GITRL structure, murine GITRL demonstrated a unique 'strand-exchanged' dimeric organization. Such a novel assembly behavior indicated a dramatic impact on receptor activation as well as on the signaling mechanism associated with the murine GITRL costimulatory system. In this present work, the 1.8 Å resolution crystal structure of murine GITRL expressed in *Drosophila melanogaster* S2 cells is reported. The eukaryotic protein-expression system allows transport of the recombinant protein into the extracellular culture medium, thus maximizing the possibility of obtaining correctly folded material devoid of any folding/assembly artifacts that are often suspected with *E. coli*-expressed proteins. The S2 cell-expressed murine GITRL adopts an identical 'strand-exchanged' dimeric structure to that observed for the *E. coli*-expressed protein, thus conclusively demonstrating the novel quaternary structure assembly behavior of murine GITRL.

1. Introduction

The members of the tumor necrosis factor (TNF) family and their receptors (TNFRs) modulate diverse biological functions, including cell proliferation, differentiation, survival and apoptosis. Conventional TNF molecules are type II membrane proteins that function as noncovalent homotrimers of β-sandwich 'jelly-roll' protomers. The TNFRs are class I membrane proteins that are characterized by ectodomains composed of pseudorepeats of one to four cysteine-rich domains. The existing structures of TNFs bound to their cognate receptors suggest a common mechanism for recognition in which a trimeric TNF assembly engages three monomeric TNFR molecules, resulting in a threefold-symmetric complex with 3:3 ligand:receptor stoichiometry. This organization directs clustering of the receptor cytoplasmic tails in a way that facilitates recruitment of the signaling adaptor proteins, such as TNF receptor-associated factors (TRAFs) and/or death domain proteins, depending on the composition of the TNFR intracellular domains as well as

the cellular context and thus resulting in activation of the downstream signaling pathways (Locksley *et al.*, 2001; Bodmer *et al.*, 2002). However, generalization of this model requires additional structural information owing to the relatively low sequence identity (~15–20%) shared by the members of the TNF/TNFR families (Bodmer *et al.*, 2002).

Glucocorticoid-induced TNF receptor (GITR) and its ligand (GITRL) are members of the TNF receptor/ligand superfamily and have been implicated in a wide range of immune functions involving both effector and regulatory T cells (Tregs; Shevach & Stephens, 2006; Nocentini *et al.*, 2007). GITR is expressed at low levels on resting mouse and human T cells, but is up-regulated upon activation of $CD4^+$ and $CD8^+$ T cells. A substantial level of GITR is constitutively expressed on $CD4^+CD25^+$ Tregs. The cognate ligand for GITR, GITRL, is expressed on several antigen-presenting cells (APCs), including macrophages, B cells and immature and mature dendritic cells. *In vivo* and *in vitro* studies on the expression profiles of GITR/GITRL suggest that GITR on activated T cells is most likely to be triggered upon engagement with GITRL expressed on APCs (Watts, 2005). In the context of suboptimal T-cell receptor stimulation, GITR engagement generates a positive costimulatory signal leading to increased T-cell proliferation and cytokine production from both $CD4^+$ and $CD8^+$ effector T cells (Ronchetti *et al.*, 2004; Stephens *et al.*, 2004; Tone *et al.*, 2003). Costimulatory effects of GITR engagement on cell proliferation and survival have also been observed on Tregs (Ji *et al.*, 2004; Kanamaru *et al.*, 2004; Ronchetti *et al.*, 2004). Most notably, GITR stimulation of effector T cells has been shown to reverse the suppressive effects of Tregs in mice (McHugh *et al.*, 2002; Shimizu *et al.*, 2002; Stephens *et al.*, 2004).

Despite the high degree of sequence identity (~50–60%) between the human and mouse orthologs of GITRL/GITR, mouse GITRL does not recognize the human receptor and human GITRL does not bind the mouse receptor (Bossen *et al.*, 2006), suggesting that these putative orthologs do not share a common mechanism for the recognition of their cognate binding partners. The GITRL–GITR signaling pathway also appears to play different roles in mice and humans (Nocentini & Riccardi, 2005), as in humans the Treg-mediated suppression of effector T-cell function is not inhibited by GITR stimulation (Levings *et al.*, 2002). In an effort to define the molecular basis of the species-specific differences in GITR–GITRL signaling, we recently characterized the structural features of human and mouse GITRL (Chattopadhyay *et al.*, 2007, 2008). Our 2.3 Å resolution X-ray crystal structure of recombinant human GITRL ectodomain expressed in *Escherichia coli* shows that like all previously characterized TNF-family members the human GITRL ectodomain self-assembles into a noncovalently associated homotrimer (Chattopadhyay *et al.*, 2007). Most remarkably, in contrast to all previously characterized TNF-family members, the 2.1 Å resolution X-ray crystal structure of mouse GITRL expressed in *E. coli* exhibited a novel dimeric assembly that is stabilized by a unique 'strand-exchange' interaction (Chattopadhyay *et al.*, 2008). The unique structural features of mouse GITRL not only support a distinct mechanism for receptor binding compared with the human ortholog, but also suggest a novel mechanism for signaling within the TNF superfamily. However, as the murine protein was expressed in *E. coli*, the possibility exists that the unique quarternary structure is the consequence of an artifact associated with heterologous expression.

Here, we report the 1.8 Å resolution crystal structure of recombinant mouse GITRL ectodomain expressed in stably transfected *Drosophila melanogaster* S2 cells. This eukaryotic system directs the secretion of recombinant mouse GITRL into the culture medium, thus maximizing the likelihood of obtaining correctly folded material. Mouse GITRL expressed in S2 cells and *E. coli* produces crystals that are nearly isomorphous and exhibit the same 'strand-exchanged' dimeric organization. These studies conclusively confirm the novel structural features of murine GITRL that are likely to impact on both mechanism and function.

2. Materials and methods

2.1. Preparation of stable *D. melanogaster* S2 cells expressing murine GITRL

The DNA sequence encoding the mouse GITRL extracellular domain (amino acids 46–173) with an N-terminal 6×His tag and Ser-Ser-Gly linker was cloned into the pMT/BiP/V5-His A expression vector (Invitrogen) between *Bgl*II and *Age*I restriction sites. A TGA stop codon was introduced at the C-terminus of the protein sequence in order to prevent C-terminal 6×His-tag expression from the vector sequence. The *Drosophila* BiP secretion signal encoded by the vector ensures efficient secretion of the recombinant protein into the extracellular culture medium of S2 cells. The resultant vector was cotransfected with the pCoBlast plasmid (at a 20:1 weight ratio) into *D. melanogaster* S2 cells using calcium phosphate (Invitrogen) as per the manufacturer's protocol. Blasticidin-resistant cells were selected for three weeks with Schneider's *Drosophila* medium with L-glutamine, supplemented with 10% heat-inactivated fetal bovine serum, 100 units ml^{-1} penicillin, 100 µg ml^{-1} streptomycin and 25 µg ml^{-1} blasticidin. Stably transfected S2 cells were analyzed for recombinant protein production in their culture medium by Western blotting using anti-His antibody (Qiagen).

2.2. Large-scale expression and purification of murine GITRL from S2 cell culture medium

For large-scale production of recombinant murine GITRL, stably transfected S2 cells were grown in EX-Cell 420 (SAFC Biosciences) supplemented with 50 µg ml^{-1} gentamycin and 2 m*M* glutamine at 298 K using a hollow-fiber bioreactor (FiberCell Systems Inc), adapting the method described in the manufacturer's manual. Briefly, 10×10^9 S2 cells (selected for stable expression of recombinant mouse GITRL) were seeded into a 20 ml capacity hollow-fiber cartridge (with a membrane of 5 kDa cutoff; FiberCell Systems Inc Catalog No. C2008) connected to a reservoir bottle containing 500 ml of the

nutrient medium described above. A continuous flow of the nutrient medium through the cartridge was maintained using a FiberCell Duet pump (FiberCell Systems Inc). Expression of the protein was induced by the addition of 0.5 m*M* $CuSO_4$ to the medium and the recombinant protein secreted into the culture supernatant within the bioreactor cartridge was harvested every alternate day. Cells were removed by centrifugation at 100*g* for 10 min at 277 K and the supernatant was further clarified by centrifugation at 5000*g* for 10 min at 277 K. The supernatant was passed through a 0.22 µm filter, exchanged into a buffer composed of 10 m*M* sodium phosphate, 150 m*M* NaCl pH 7.4 and was supplemented with 10 m*M* imidazole. The 6×His-tagged murine GITRL was purified from the culture supernatant by affinity chromatography using Ni–NTA agarose (Qiagen) and gel-filtration chromatography on Superdex 200.

2.3. Protein deglycosylation with PNGase F

Murine GITRL purified from the S2 cell-culture supernatant showed two bands on reducing SDS–PAGE corresponding to differently glycosylated forms of the recombinant protein (Fig. 1*a*). For enzymatic deglycosylation under nondenaturing conditions, 1 mg purified mouse GITRL in 10 m*M* sodium phosphate, 150 m*M* NaCl pH 7.4 was incubated with 2500 units of PNGase F for 18 h at 310 K. More than 95% of the protein was deglycosylated as demonstrated by SDS–PAGE analysis under reducing conditions (Fig. 1*a*).

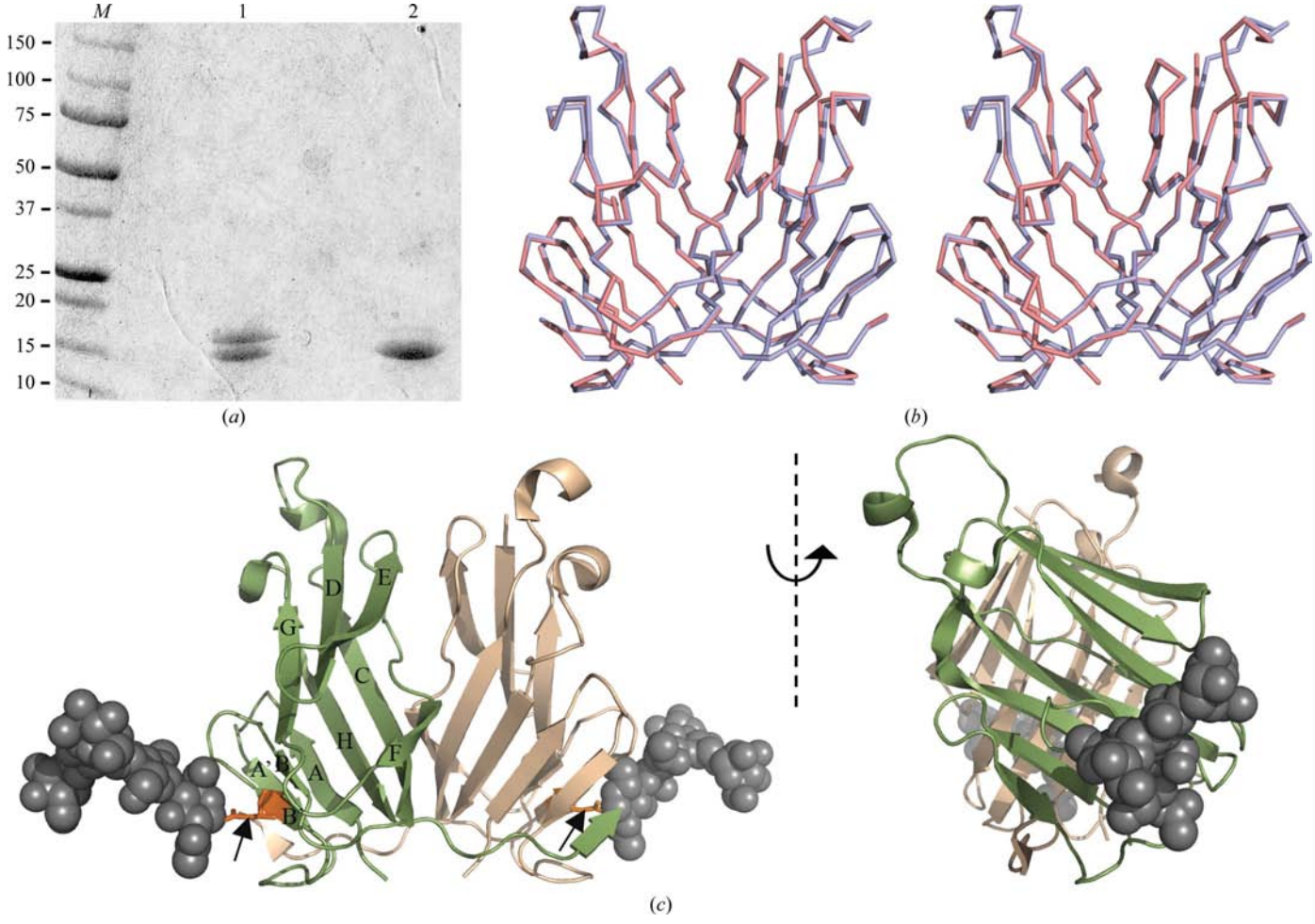

Figure 1
The crystal structure of recombinant mouse GITRL isolated from *D. melanogaster* S2 cells shows a twofold-symmetric dimer similar to that observed in the crystal structure of *E. coli*-expressed mouse GITRL (PDB code 2qdn). (*a*) A Coomassie-stained reducing SDS–PAGE of mouse GITRL purified from *D. melanogaster* S2 cell-culture supernatant showed two bands corresponding to differently glycosylated forms of the protein (lane 1). Treatment with PNGase F under nondenaturing condition led to deglycosylation of >95% of the protein (lane 2) and resulted in a homogeneous preparation of the sample that was suitable for X-ray crystallographic studies. Molecular-weight standards (lane *M*) were included for comparison. (*b*) A stereoview of the superposition of the S2 cell-expressed mouse GITRL dimer (PDB code 3fc0; light red) on *E. coli*-expressed mouse GITRL dimer (2qdn; light blue) shows remarkable structural agreement between the two crystal structures, thus confirming the novel dimeric organization of mouse GITRL within the TNF superfamily. (*c*) A ribbon representation shows that the two classical β-sandwich 'jelly-roll' subunits (shown in green and wheat) of the mouse GITRL dimer are associated in a unique fashion, making an angle of $\sim$40° with respect to each other. Ten antiparallel β-strands are labeled. The C-terminal end of each chain swaps with the other chain to form a novel 'strand-exchanged' dimer. The potential *N*-glycosylation sites at Asn74 (orange sticks) of both chains are indicated by black arrows. The *in silico* model of basic *N*-glycan moieties (gray spheres) shows no possible interference of the *N*-glycan moiety with either the dimer interface or the 'strand-exchanged' region of the protein.

Table 1
Crystallographic data and refinement statistics.

Values in parentheses are for the high-resolution data bin.

PDB code	3fc0
Source	NSLS X29A
Wavelength (Å)	0.97910
Resolution limits (Å)	30–1.75
Space group	$P2_12_12_1$
Unit-cell parameters (Å)	a = 52.61, b = 69.29, c = 73.99
No. of observations	200650
No. of unique reflections	27166
Completeness (%)	99.4 (95.3)
Mean $I/\sigma(I)$	33.85 (5.73)
$R_{\rm merge}$ on I†	5.1 (30.4)
Cutoff criterion $I/\sigma(I)$	0
Refinement statistics	
Resolution limits (Å)	30.00–1.76
No. of reflections	27086
Cutoff criterion $I/\sigma(I)$	0
Protein/water atoms	1932/92
$R_{\rm cryst}$‡	0.22 (0.25)
$R_{\rm free}$ (5% of data)	0.26 (0.29)
R.m.s.d.s	
Bonds (Å)	0.02
Angles (°)	1.54
B factors (Å^2)	
Main chain	1.04
Side chains	2.79

† $R_{\rm merge} = \sum_{hkl}\sum_i |I_i(hkl) - \langle I(hkl)\rangle|/\sum_{hkl}\sum_i I_i(hkl)$. ‡ $R_{\rm cryst} = \sum_{hkl} |F_{\rm o}(hkl) - |F_{\rm c}(hkl)|/\sum_{hkl} |F_{\rm o}(hkl)|$, where $F_{\rm o}$ and $F_{\rm c}$ are observed and calculated structure factors, respectively.

2.4. Crystallization, data collection and structure determination

Deglycosylated mouse GITRL purified from S2 cells was concentrated to 3 mg ml^{-1} in buffer containing 10 m*M* Tris pH 8.5 and 10 m*M* NaCl. The protein was crystallized by sitting-drop vapor diffusion at room temperature with a 1:1 mixture of protein solution and precipitant composed of 15%(*v*/*v*) Tacsimate pH 7.0, 0.1 *M* HEPES pH 7.0 and 2%(*w*/*v*) polyethylene glycol 3350. Data were collected to a resolution of 1.8 Å on beamline X29A at the National Synchrotron Light Source (NSLS). The data were integrated and scaled with *HKL*-2000 (Otwinowski & Minor, 1997) and were consistent with space group $P2_12_12_1$ with unit-cell parameters a = 52.609, b = 69.293, c = 73.994 Å (with two molecules in the asymmetric unit). The structure was solved by molecular replacement using the program *Phaser* (McCoy *et al.*, 2007) from the *CCP*4 suite (Collaborative Computational Project, Number 4, 1994) with the *E. coli*-expressed refolded mouse GITRL protein structure (PDB code 2qdn; space group $P2_12_12_1$, unit-cell parameters a = 52.92, b = 71.51, c = 70.19 Å; Chattopadhyay *et al.*, 2008) as the search model. The model was improved by manual revision with the program *Coot* (Emsley & Cowtan, 2004) and refinement with *REFMAC*5 (Murshudov *et al.*, 1997). Data-collection and refinement statistics are shown in Table 1.

2.5. Analysis of the structure

Structural superpositions were performed with *Coot* (Emsley & Cowtan, 2004) and the *CCP*4 suite (Mitchell *et al.*, 1990; Potterton *et al.*, 2002, 2004) and accessible surface areas and atomic contacts were calculated with the *AREAIMOL* (Lee & Richards, 1971) and *CONTACT* programs from the *CCP*4 suite (Collaborative Computational Project, Number 4, 1994), respectively. Ribbon diagrams, atomic models and electron-density representations were generated by *PyMOL* (http://www.pymol.org). The potential site of *N*-glycan modification was predicted with the *NetNGlyc* 1.0 server (http://www.cbs.dtu.dk/services/NetNGlyc/). An *in silico* glycosylation model of the protein was built using the *Glyprot* web server (http://www.glycosciences.de/glyprot/; Bohne-Lang & von der Lieth, 2005).

3. Results and discussion

We previously reported the crystal structures of human and mouse GITRL expressed in *E. coli* (Chattopadhyay *et al.*, 2007, 2008). Unlike all known TNF molecules, including human GITRL, our mouse GITRL crystal structure showed a novel 'strand-exchanged' dimer that had not previously been observed for any other member of the TNF family. Here, we provide further support for this novel dimeric assembly behavior by determining the crystal structure of recombinant murine GITRL secreted by *D. melanogaster* S2 cells. This strategy allows expression in a eukaryotic system and directs the secretion of glycosylated recombinant protein into the extracellular culture medium, thus maximizing the likelihood of obtaining correctly folded material. Purified mouse GITRL isolated from the S2 cell-culture medium also exhibited receptor-binding activity similar to that of *E. coli*-expressed material (Chattopadhyay *et al.*, 2008).

Purified mouse GITRL expressed from S2 cells migrated on SDS–PAGE as two bands corresponding to differently glycosylated forms of the recombinant protein (Fig. 1*a*). To achieve homogeneity in the protein sample for crystallization purposes, we subjected this S2 cell-expressed mouse GITRL to enzymatic deglycosylation under native conditions with PNGase F. Such treatment led to at least >95% deglycosylation of the more highly glycosylated state of the protein, resulting in enrichment of the less glycosylated form of the protein (Fig. 1*a*). This PNGase F-treated protein was subsequently used in crystallization experiments.

The crystal structure of deglycosylated mouse GITRL expressed in S2 cells was determined by molecular replacement and refined to a resolution of 1.8 Å. The asymmetric unit contained two polypeptide chains (chain *A* and chain *B*), which superpose with an r.m.s.d. of 0.48 Å over 119 C$^\alpha$ atoms. The quality of the electron density corresponding to the N-terminal 14 residues (His_6-Ser-Ser-Gly plus Pro46–Glu50) from both chains and the Lys104–Ala107 region of chain *B* was poor and these segments were omitted from the final model. Consistent with complete removal of the glycosylation moiety upon PNGase F treatment, no density for any carbohydrate group could be detected near the potential glycosylation site at position Asn74.

As observed in our previously determined 2.1 Å crystal structure of mouse GITRL expressed in *E. coli* (PDB code 2qdn), the present crystal structure of the protein isolated

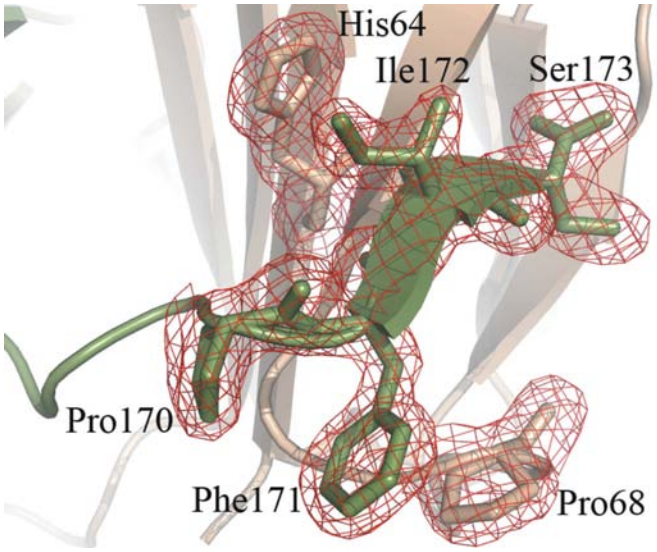

Figure 2
$2F_o - F_c$ density maps (red) centered on the 'strand-exchange' region of S2 cell-expressed mouse GITRL dimer. The C-terminal Pro170-Phe171-Ile172-Ser173 segment from one subunit forms a unique 'strand-swap' with the other subunit. This strand-swap appears to be stabilized through strong hydrophobic/stacking interactions that involve Pro170, Phe171 and Ile172 from the C-terminus of one chain (pale green) and His64 (A' strand) and Pro68 ($A'B'$ loop) of the neighboring chain (light orange). The $2F_o - F_c$ map is contoured at the 1σ level and density within a radius of 1.6 Å of the model is displayed.

from S2 insect cells exhibits a 'strand-exchanged' dimeric assembly of β-sandwich 'jelly-roll' protomers (Figs. 1*b* and 1*c*). The two dimeric structures are highly similar, with an r.m.s.d. of 0.32 Å over 242 C^{α} atoms (Fig. *b*). Further comparison of the two crystal structures shows similar buried surface areas at the interfaces between the engaging monomers (~3016 Å^2 in the present structure and ~2998 Å^2 in 2qdn). In addition, the patterns of hydrogen-bond formation at the dimer interfaces of the two structures remain almost consistent. In the 2qdn structure 12 residues contribute 16 potential hydrogen bonds at the subunit interface. In the current structure, the same set of residues, apart from Met124 and Gln128, are involved in the formation of 15 potential hydrogen bonds.

Consistent with the previous bacterially expressed protein structure 2qdn, the current structure also shows that the C-terminal end (Pro170-Phe171-Ile172-Ser173) of each subunit swaps in a unique fashion with the other subunit and generates a series of hydrophobic/stacking interactions involving His64 on the A' strand and Pro68 on the $A'B'$ loop of the other subunit (Fig. 2). Our previous mutagenesis data have shown that this 'strand-exchange' interaction acts as a major stabilizing force for the dimeric assembly of mouse GITRL (Chattopadhyay *et al.*, 2008).

4. Conclusion

In this work, we have determined the 1.8 Å resolution X-ray crystal structure of mouse GITRL protein recombinantly produced from *D. melanogaster* S2 cells. This expression system results in the secretion of soluble mouse GITRL protein from S2 cells into the extracellular culture medium, ensuring correct folding of the recombinant protein and thus excluding the possibility of artifacts associated with bacterial expression and refolding. S2 cell expression also allowed the incorporation of a single simple glycan moiety (nearly 1 kDa) at the potential *N*-glycosylation site at position Asn74. This potential *N*-glycosylation site is located at a distal position from the dimer interface of mouse GITRL (Fig. 1*c*) and therefore does not seem to interfere with the dimeric organization of the protein. The glycan moiety could be efficiently removed by PNGase F treatment, thus improving the homogeneity of the protein for X-ray crystallographic studies. Compared with our previous bacterially expressed protein structure 2qdn, the current structure shows no significant change in local or global structure and conformation and, most importantly, it exhibits the same novel 'strand-swapped' dimeric organization that has not been previously reported for any other member of the TNF-ligand superfamily. Structural characterization of S2 cell-expressed mouse GITRL confirms the novel dimeric organization of the protein as a remarkable exception to the common trimeric paradigm for TNF molecules and strengthens our hypotheses that mouse GITRL employs a novel receptor-activation mechanism that has not been appreciated for other TNF-family members.

We gratefully acknowledge the staff of the X29A beamline at the National Synchrotron Light Source and Rafael Toro for assistance with protein crystallization. This work was supported by the National Institutes of Health Grants 5RO1AI07289 (SGN and SCA), Cancer Center Support Grant (P3OCAO13330) and a postdoctoral fellowship from the Cancer Research Institute (KC).

References

Bodmer, J. L., Schneider, P. & Tschopp, J. (2002). *Trends Biochem. Sci.* **27**, 19–26.
Bohne-Lang, A. & von der Lieth, C. W. (2005). *Nucleic Acids Res.* **33**, W214–W219.
Bossen, C., Ingold, K., Tardivel, A., Bodmer, J. L., Gaide, O., Hertig, S., Ambrose, C., Tschopp, J. & Schneider, P. (2006). *J. Biol. Chem.* **281**, 13964–13971.
Chattopadhyay, K., Ramagopal, U. A., Brenowitz, M., Nathenson, S. G. & Almo, S. C. (2008). *Proc. Natl Acad. Sci. USA*, **105**, 635–640.
Chattopadhyay, K., Ramagopal, U. A., Mukhopadhaya, A., Malashkevich, V. N., DiLorenzo, T. P., Brenowitz, M., Nathenson, S. G. & Almo, S. C. (2007). *Proc. Natl Acad. Sci. USA*, **104**, 19452–19457.
Collaborative Computational Project, Number 4 (1994). *Acta Cryst.* D**50**, 760–763.
Emsley, P. & Cowtan, K. (2004). *Acta Cryst.* D**60**, 2126–2132.
Ji, H. B., Liao, G., Faubion, W. A., Abadia-Molina, A. C., Cozzo, C., Laroux, F. S., Caton, A. & Terhorst, C. (2004). *J. Immunol.* **172**, 5823–5827.
Kanamaru, F., Youngnak, P., Hashiguchi, M., Nishioka, T., Takahashi, T., Sakaguchi, S., Ishikawa, I. & Azuma, M. (2004). *J. Immunol.* **172**, 7306–7314.
Lee, B. & Richards, F. M. (1971). *J. Mol. Biol.* **55**, 379–400.
Levings, M. K., Sangregorio, R., Sartirana, C., Moschin, A. L., Battaglia, M., Orban, P. C. & Roncarolo, M. G. (2002). *J. Exp. Med.* **196**, 1335–1346.

Locksley, R. M., Killeen, N. & Lenardo, M. J. (2001). *Cell*, **104**, 487–501.
McCoy, A. J., Grosse-Kunstleve, R. W., Adams, P. D., Winn, M. D., Storoni, L. C. & Read, R. J. (2007). *J. Appl. Cryst.* **40**, 658–674.
McHugh, R. S., Whitters, M. J., Piccirillo, C. A., Young, D. A., Shevach, E. M., Collins, M. & Byrne, M. C. (2002). *Immunity*, **16**, 311–323.
Mitchell, E. M., Artymiuk, P. J., Rice, D. W. & Willett, P. (1990). *J. Mol. Biol.* **212**, 151–166.
Murshudov, G. N., Vagin, A. A. & Dodson, E. J. (1997). *Acta Cryst.* D**53**, 240–255.
Nocentini, G. & Riccardi, C. (2005). *Eur. J. Immunol.* **35**, 1016–1022.
Nocentini, G., Ronchetti, S., Cuzzocrea, S. & Riccardi, C. (2007). *Eur. J. Immunol.* **37**, 1165–1169.
Otwinowski, Z. & Minor, W. (1997). *Methods Enzymol.* **276**, 307–326.
Potterton, E., McNicholas, S., Krissinel, E., Cowtan, K. & Noble, M. (2002). *Acta Cryst.* D**58**, 1955–1957.
Potterton, L., McNicholas, S., Krissinel, E., Gruber, J., Cowtan, K., Emsley, P., Murshudov, G. N., Cohen, S., Perrakis, A. & Noble, M. (2004). *Acta Cryst.* D**60**, 2288–2294.
Ronchetti, S., Zollo, O., Bruscoli, S., Agostini, M., Bianchini, R., Nocentini, G., Ayroldi, E. & Riccardi, C. (2004). *Eur. J. Immunol.* **34**, 613–622.
Shevach, E. M. & Stephens, G. L. (2006). *Nature Rev.* **6**, 613–618.
Shimizu, J., Yamazaki, S., Takahashi, T., Ishida, Y. & Sakaguchi, S. (2002). *Nature Immunol.* **3**, 135–142.
Stephens, G. L., McHugh, R. S., Whitters, M. J., Young, D. A., Luxenberg, D., Carreno, B. M., Collins, M. & Shevach, E. M. (2004). *J. Immunol.* **173**, 5008–5020.
Tone, M., Tone, Y., Adams, E., Yates, S. F., Frewin, M. R., Cobbold, S. P. & Waldmann, H. (2003). *Proc. Natl Acad. Sci. USA*, **100**, 15059–15064.
Watts, T. H. (2005). *Annu. Rev. Immunol.* **23**, 23–68.